Investigating the Impact of Deposition Power on PVD Growth WS_2 for Solar Cell Application

K. Sobayel[1], Nurhafiza.K[2], Md. Akhtaruzzaman[2], Afida Ayob[1], N.Amin[4]
[1]Department of Electrical Electronic & Systems Engineering, FKAB, Universiti Kebangsaan Malaysia, Bangi, Selangor, Malaysia.
[2]General and Pre-University Study, German Malaysian Institute, 43000, Kajang, Selangor, Bangi, Malaysia.
[3]Solar Energy Research Institute, Universiti Kebangsaan Malaysia, Bangi, Malaysia.
[4]Institute of Sustainable Energy, Universiti Tenaga Nasional, Putrajaya, Malaysia
sobayel@siswa.ukm.edu.my, nurhafiza@gmi.edu.my, akhtar@ukm.edu.my, Afida.ayob@ukm.edu.my, nowshad@uniten.edu.my*

***Abstract*— Physical Vapor Deposition (PVD) was used to grow ultra-thin tungsten di sulfide (WS_2) layers on top of soda lime glass substrates. Deposition power of radio frequency magnetron sputtering was varied (50W, 100 W, 150 W,200 W and 250 W) to study its impact on film characteristics for suitable application in solar cell. Structural, morphological and opto-electrical properties of as grown film were analyzed. Optimized monocrystalline ultra-thin WS_2 films of enhance crystallite (690 nm thick) were successfully hoarded with RF power of 150 W under 100°C temperature.**

Keywords—Tungsten di sulfide (WS_2), thin film, sputtering, solar cell.

I. INTRODUCTION

Transitional metal dichalcogenides (TMDCs) have been promising for a wide array of applications for decades, but due to their excellent performance in demanding applications sudden attention was given. Among the candidates of the solar cells, thin film solar cells especially inexpensive, abundant and nontoxic material tungsten di sulfide (WS_2) has attracted an increasing interest in this arena. Due to its layered structure, its optical and electrical properties are strongly anisotropic. Although single crystals have been extensively studied for optical devices, only a few studies on the photovoltaic characteristics of thin films have been performed. TMDCs MoS_2 and WS_2 in specific raised particular interests for the photovoltaic community in thin film solar cells as absorber layer material [1, 2]. This is due to their suitable bandgaps (1-2 eV) and the very high absorption coefficients which is over 105 cm–1 [3,4]

The development of WS_2 in thin film solar cell is still in its infancy compared to other types of solar cell materials like Si, CdTe, CZTS, CIGS etc. Presently the major driving force in solar photovoltaic is silicon solar cell technology followed by CdTe and CIGS respectively. But the production cost of Si solar technology is quite high. Moreover, the scarcity of indium supply, high material cost of gallium and toxicity problem imposed by Cd and Te impelled researchers to look for a low cost, nontoxic and earth abundant material for photovoltaic applications. Approximately 30 years in the past, TMDCs have been examined as semiconductors for solar cells with a liquid electrode [3, 5,6]. TMDC thin films for photovoltaic application` were grown by a variety of methods. At least two groups have deposited WS_2 and MoS_2 by chemical vapor deposition (MOCVD). In both cases, MoS_2 films exhibited good photoconductivity, while WS_2 did not. WS_2 layer deposited by R.F magneto sputtering does not appear good crystalline structures but was uniformly deposited. WS_2 films were also deposited from tungsten by sulfurization [10, 11] or sulfurizing tungsten oxide films [7, 12] or from tungsten targets by reactive magnetron sputtering method in Ar/H_2S atmosphere [8, 13, 14], electrodeposition and chemical vapor deposition [15].

The PVD describes a number of vacuum deposition methods, for the production of thin films and coatings. Physical vapor deposition (PVD) PVD has a process wherein the material is transported from a condensed stage to a steam phase and then back to the condensed phase of a thin film. Among all the deposition techniques; Physical Vapor Deposition (PVD) technique like RF magnetron sputtering has got some distinct advantages from others [16,17]:

- It requires lower temperatures of the substratum in comparison with methods of thermally activated deposition,
- High thermodynamic properties of the species due to plasma-assisted dissociation and excitement,
- Compact and dense,
- well adhering film can be prepared for deposition of compounds and alloys.

Last but not least, reactive magnetron sputtering is a well-established method of large-scale deposition, enabling substratum sizes of 3 to 6 m^2, for example for architectural glass coating[18,19]. It would be a technical breakthrough to use this large-scale deposition technique to prepare thin-film solar cells that need to be produced in a year [20]. For the different layers in thin film solar cells device structure, e.g., for metal back contacts (Mo, Ag) [21] or copper / gallium and indium metal precursor layers for Cu (In, Ga) $S(Se)_2$ absorbers[22,23] or transparently conductive oxides (ZnO, ITO) [24-26]; magnetrons techniques are already widely used for deposition. But it has to bear in mind that sputtering RF magnetron is a process of deposition assisted by plasma or ion that bombards atoms to substrates for growing film. Fluctuations in the structure and bonding of the deposited material tend to occur due to this high energetic bombardment of atoms. This can result in both beneficial and detrimental photovoltaic application effects. For this reason, deposition parameters such as temperature, power, target-substrate distance, etc. play a significant role in sputtering in the preferential growth process, so it is

978-1-5386-8394-1/19/$31.00 ©2019 IEEE

Authorized licensed use limited to: UNIVERSITY TENAGA NASIONAL. Downloaded on November 24,2021 at 02:26:28 UTC from IEEE Xplore. Restrictions apply.

crucial to optimize proper WS_2 parameters for photovoltaic application.

With a view to suitable application of WS_2 in solar cell, this paper has extensively studied morphological and optoelectrical properties of optimized WS_2 deposited by rf magnetron sputtering technique. Hence, this study mainly investigated the effects of deposition power on the structural, surface morphology and electrical properties of RF sputtered WS_2 film. The study also focuses to eliminate pinholes on sputtered film.

II. METHODOLOGY

A. Experimental Methods

WS_2 thin film is deposited by Physical Vapor Deposition (RF magnetron sputter deposition process) technique under high vacuum atmosphere. Soda lime glass substrates of 7.5 cm × 2.5 cm × 0.2 cm were used for film deposition. They were pre-cleaned in ultrasonic bath by sequential cleaning process (mechanical scrubbing–acetone–methanol–deionized water) and dried with N_2 gas flow. A 50 mm diameter WS_2 (99.99%) sputtering target (Kurt. J. Lesker) was used as source material. Initial purging of sputtering chamber and Pre-sputtering were carried out for 15 min with 50 W power to remove unwanted components from the chamber. Deposition chamber base pressure was brought down to 10^{-4} Pa by turbo-molecular pump and the working pressure during all the deposition run was maintained at 1.5 Pa by flowing 4 sccm of purified Ar (99.99%) as the working gas into the chamber. Target to substrate distance (sputter down) and substrate holder rotation were fixed at 8 cm and 10 rpm respectively. Deposition parameters used for this study are shown in table 1. During the deposition process, substrate temperature fixed at 100°C. All the samples were kept inside upon completion of deposition until substrate temperature falls to room temperature. This also facilitates as grown samples of being oxidized.

B. Film Charecterizations

BRUKER αXS-D8 Advance CuKα diffractometer examined the structural and crystallinity properties as well as the crystal orientation along the normal surface of the film. XRD patterns were recorded in the 2Θ range from 10° to 80° with a step size of 0.05° using Cu Kα radiation wavelength, λ= 1.5408˚A. The mean crystallite sizes (D) of the films was calculated using Scherrer formula. Atomic force microscopy (AFM) was used to study a variety of surface effects present in embossed structures. Using Carl Zeiss Merlin field emission scanning electron microscope (FESEM) operated at 3 kV, grain size, surface morphology and cross-sectional view were observed. Opto-electrical properties such as carrier concentration, mobility, and resistivity were measured by Hall Effect measurement system, HMS ECOPIA 3000 with a magnetic field of 0.57 T and probe current of 100 nA for all the samples. Tauc plot is used to calculate the absorption coefficient and band gaps. Pinholes were observed and adhesiveness of the film was tested.

TABLE I: SPUTTERING PARAMETERS

Parameter	Condition
Target	WS_2 (99.9% pure)
Substrate	Soda Lime Glass
Base Pressure	3.0×10^{-6} Torr
Working Pressure	2.1×10^{-2} Torr
Deposition Time	15 min
Growth Temperature	100°C
RF Power	50 W, 100 W, 150 W, 200 W & 250 W
Gas & Flow Rate	Argon (4.0 sccm)

III. RESULTS AND DISCUSSION

A. Adhesiveness of Films

Adhesiveness is a primary requirement for any deposition on substrate. Scotch-tape method is very effective to check adhesiveness of any film [27]. Scotch tape test usually conducted on samples immediately after deposition process; here it was performed after the completion of natural cooling of substrates. Thickness of as grown films were measured from cross-sectional image by using FESEM. Table II shows the outcome of Scotch tape test with respect to different powers. It has been observed that most of the films had shown good adherence to the SLG substrates except the film deposited with high power. Some elemental WS_2 has been observed while deposition is done with 250 W. By default, sputtering is the process of bombardment of particles with high energy. A threshold energy for the release of an atom from the target exists, below which the atom is not "sputtered". The yield increases with the application of deposited power. At very high energies, the yield decreases because of the increasing penetration depth and hence increasing energy loss below the surface. When more higher inputs of power are added with its default energy, it causes the bombarded particles bounce back from the substrates. Thereby reduces adhesiveness of the film [28].

B. Pinhole Reduction

Pinholes are best seen by illuminating the metallic film from behind, sometimes referred to as pin-windows. The metallic film will attenuate the light when viewed from the front except for a scattering of bright light pinpricks. The pinpricks of light are often almost circular in shape where there is an area of unmetallized film. These unmetallized areas are caused primarily by dust or scrap metallized on the surface when the film passes through the deposition area, but sometimes after moving the scrap so that the remaining area is an unmetallized one corresponding to the shadow shape of the scrap. Occasionally the debris does not roll away but slides away, so that the pinhole can also have a scratch track that leads away from the unmetallized area. Mostly they are two types: natural and artificial. Natural pinholes, which occur very rarely, are very difficult to eliminate as they come with material from the material. But artificial pinholes can be eliminated by easily by using different techniques. Figure 1 (a) and (b) demonstrate films with pinhole and without pinhole respectively. Figure 1(c) exhibits the pinhole engineering inside the sputtering chamber. In this

Authorized licensed use limited to: UNIVERSITY TENAGA NASIONAL. Downloaded on November 24,2021 at 02:26:28 UTC from IEEE Xplore. Restrictions apply.

experiment, pinholes are effectively removed by changing substrate to target distance from 8 cm to 10.6 cm.

TABLE II: THICKNESS AND ADHESIVENESS OF WS_2 FILM

Sputtering Target	Deposition Power(W)	Film Thickness (nm)	Scotch-tape Test
WS_2	50	153.6	Pass
	100	361	Pass
	150	692.2	Pass
	200	789	Pass
	250	908.1	Partially Pass

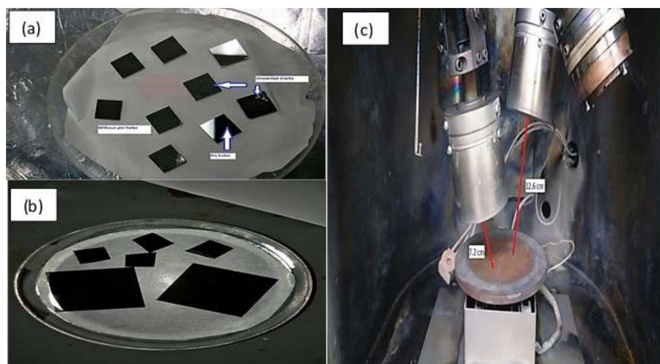

Fig 1: (a) Films with pinholes (b) films without pinholes after fixing optimized target-substrate distance (c) Physical view of pinhole reduction engineering

C. *Structural Properties*

Figure 2 shows the XRD pattern for as-sputtered WS_2 films of different powers where 2ϴ angle ranges from 10◦ to 80◦. All films exhibited two primary peaks of (101) and (112) orientations. indicating polycrystalline nature of the as-sputtered and annealed Mo films. The obtained XRD patterns of this study agree with the standard XRD pattern documented in JCPDS card. All the films are in 2H phase which is suitable for semiconducting applications [29]. It also exhibits that most intense peak is at 2ϴ = 33.8◦ corresponding to (101) preferred orientation. The highest peak has been found with two deposition powers- 50W and 150 W. Peak width (β) is inversely proportional to crystallite size (D). β value is almost same for all variations. The results of X-Ray Diffraction (XRD) measurements are shown in Table III. The average particle size or grain size was calculated from the broadening of the (101) peak using Scherrer equation.

$$L = \frac{K\lambda}{B\ \cos\theta}$$

Where K, L, λ , B, θ are the Scherrer constant, grain size, wavelength of the X-ray source, and full width half maximum, and diffraction angle, respectively. Grain size has been calculated and ranges from 93.97 Ǎ to 62.43 Ǎ.

Moreover, lower value of strain signifies higher crystallinity [31]. Figure 3 shows the changes of crystallinity and strain

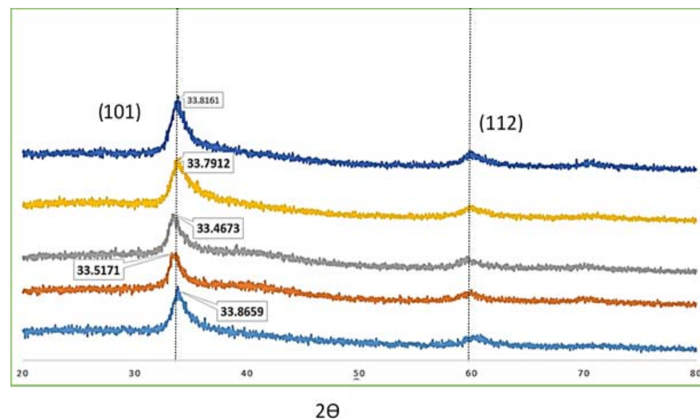

Fig 2: XRD patterns for various deposition power (bottom to up: 50W TO 250 W)

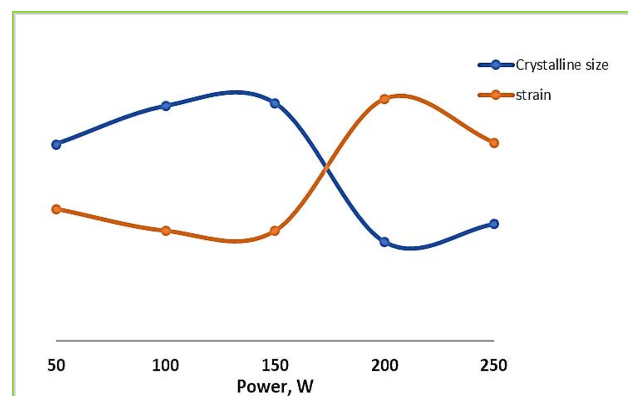

Fig 3: Comparative view of film crystallinity and strain with respect to sputtering power

with respect to different deposition power. Here it is observed that at lower deposition power films exhibits crystallinity and best result observed at 150W. With the increase of power higher than 150W, films crystallinity decreases, and strain increases which are not suitable for photovoltaic applications.

D. *Surface Morphology*

A Field Emission Scanning Electron Microscopy (FESEM) images of WS_2 thin films presented in figure 4 divulge the surface morphologies of sputtered WS_2 thin films at different deposition powers. Literature review indicates that films sputtered at lower deposition power exhibited porous microstructures while films sputtered at higher deposition power exhibited dense microstructures [30, 32].

Authorized licensed use limited to: UNIVERSITY TENAGA NASIONAL. Downloaded on November 24,2021 at 02:26:28 UTC from IEEE Xplore. Restrictions apply.

TABLE III: STRUCTURAL MEASUREMENT ANALYSIS FROM XRD OF WS_2 THIN FILMS

Power	d Values (calculated) Å	Peak Θ in deg	FWHM (ß)	Grain size Å	Strain (ε)
50	2.644	16.93	0.0171	84.72	0.014
100	2.671	16.75	0.0155	93.38	0.013
150	2.674	16.73	0.0154	93.97	0.013
200	2.649	16.89	0.0232	62.43	0.019
250	2.645	16.90	0.0217	66.54	0.017

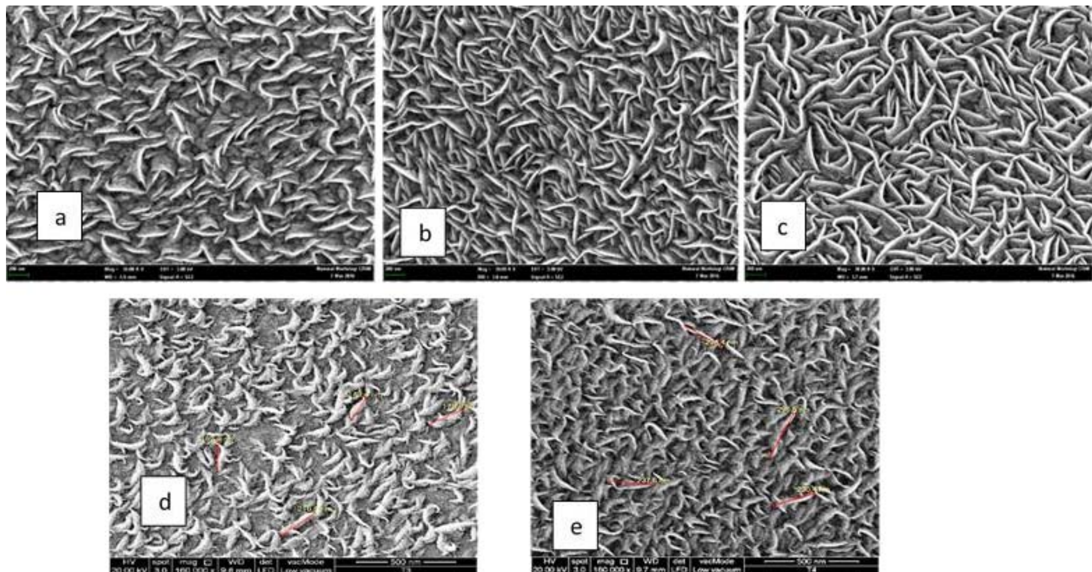

Fig 4: Fesem image of as deposited WS_2 under different sputtering power (A TO E: 50 W TO 250 W)

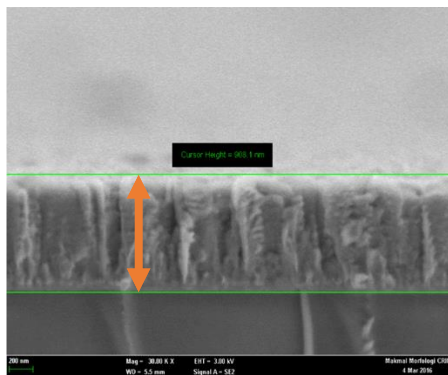

Fig 5: Cross-sectional image of WS_2 with 150W deposition power

At higher deposition power, deposition rate increases so that number of particles received at the substrate increases resulting in a denser microstructure while at low deposition power, deposition rate decreases and the number of species arriving at the surface of the substrate becomes less resulting in a porous microstructure [33]. But here, this phenomenon is applicable up to 150 W; beyond this power, films lose its crystallinity which is also found from XRD analysis for WS_2. However, in case of WS_2 no porous microstructure was observed. It also shows a smooth morphology and revealing dense microstructure for all variations of power. The cross-

Authorized licensed use limited to: UNIVERSITY TENAGA NASIONAL. Downloaded on November 24,2021 at 02:26:28 UTC from IEEE Xplore. Restrictions apply.

sectional view (Fig 5) of the WS_2 thin films deposited shows granular morphology.

IV. Conclusion

WS_2 thin film deposited by RF magnetron sputtering by varying power were carefully studied. All the efforts are given to optimize the sputtering parameter for suitable photovoltaic applications. To do so, pinhole reduction engineering was made, and adhesives test was also conducted. Moreover, physical and morphological properties of WS_2 thin films deposited by PVD method were also investigated. The effects of deposition power on film microstructure, strain and crystallinity of WS_2 thin films were scrutinized. For the range of synthesis conditions investigated, deposited films were found to exhibit single diffraction peak corresponding to (101) plane. Film morphology was found to be very smooth with granular morphology. Finally, it is established that 50W~150W is the optimized deposition power for RF magnetron sputtering for WS_2 thin film deposition.

V. Reference

[1] R. G. Dickinson and L. Pauling, J. Am. Chem. Soc. 45, 1466 (1923).

[2] R. G. W. Wyckoff, Crystal Structures (Inter science, New York, 1963).

[3] H. Tributsch, Ber. Bunsenges. Phys. Chem. 81, 362 (1977).

[4] H. J. Lewerenz, A. Heller, and F. J. Di Salvo, J. Am. Chem. Soc. 102, 1877 (1980).

[5] E. Bucher, “Photo electrochemistry and Photovoltaics of Layered Semiconductors”, edited by A. Aruchamy (Kluwer Academic Publishers, Dordrecht, 1992

[6] K. Sobayel et al, “Numerical modeling of high efficiency tungsten-di-sulfide (WS_2) Solar Cells with Various Buffer Layers By Scaps-1D”, Chalcogenide Letters, Vol. 15, No. 6, (2018)

[7] A. Matthäus, A. Ennaoui, S. Fiechter, T. Kiesewetter, K. Diesner, I. Sieber, W. Jaegermann, T. Tsirlina, and R. Tenne, J. Electrochem. Soc. 144, 1013 (1996).

[8] M. Regula, C. Ballif, and F. Lévy, “Polycrystalline semiconductors IV – Physics, Chemistry and Technology”, edited by S. Pizzini, H. P. Strunk, and J. H. Werner (Trans Tech, Zug, Switzerland, 1995) p. 335.

[9] Sèmeh Jebli et al., “Synthesis, crystal structure, Mössbauer spectroscopy, optical and magnetic properties of $Cs_2M_2Fe(PO_4)_3$ (M = Mn, Co, Ni, Cu) ordered pollucite structure”, Journal of Solid State Chemistry, Volume 270, February 2019, Pages 265-272.

[10] A. K. Rai, R. S. Bhattacharya, J. S. Zabinski, and K. Miyoshi, Surf. Coat. Technol. 92, 120 (1997).

[11] M. Genut, L. Margulis, G. Hodes, and R. Tenne, Thin Solid Films 217, 91 (1992).

[12] A. Jäger-Waldau, M. C. Lux-Steiner, G. Jäger-Waldau, and E. Bucher, Appl. Surf. Sci. 70/71, 731 (1993).

[13] Y. Feldman, G. L. Frey, M. Homyonfer, V. Lyakhovitskaya, L. Margulis, H. Cohen, G. Hodes, J. L. Hutchinson, and R. Tenne, J. Am. Chem. Soc. 118, 5362 (1996).

[14] K. Ellmer, C. Stock, K. Diesner, and I. Sieber, J. Cryst. Growth 182, 389 (1997).

[15] K. Ellmer, R. Mientus, S. Seeger, and V. Weiß, phys. stat. sol. (a) 201, R97 (2004).

[16] C. J. Carmalt, I. P. Parkin, and E. S. Peters, Polyhedron 22, 1499 (2003).

[17] V. Buck, Thin Solid Films 198, 157 (1991).

[18] K. Ellmer, “Low temperature plasmas. fundamentals, technologies and techniques”, Vol. 2, edited by R. Hippler,H. Kersten, M. Schmidt, and K. H. Schoenbach (Wiley-VCH, Berlin, 2008), p. 675. J. Szczyrbowski, G. Bräuer, M. Ruske, H. Schilling.

[19] A. Zmelty, Thin Solid Films 351, 254 (1999).

[20] H. Ohsaki and Y. Kokubu, Thin Solid Films 351, 1 (1999).

[21] K. Zweibel, J. Mason, and V. Fthenakis, Sci. Am. Mag. 298, 48 (2008).

[22] K. Orgassa, H. W. Schock, and J. H. Werner, Thin Solid Films 431/432, 387 (2003).

[23] J. Klaer, K. Siemer, I. Luck, and D. Bräunig, Thin Solid Films 387, 169 (2001).

[24] V. Probst, W. Stetter, W. Riedl, H. Vogt, M. Wendl, H. Calwer, S. Zweigart, K.-D. Ufert, B. Freienstein, H. Cerva, and F. H. Karg, Thin Solid Films 387, 262 (2001).

[25] O. Kluth, G. Schöpe, B. Rech, R. Menner, M. Oertel, K. Orgassa, and H. W. Schock, Thin Solid Films 502, 311 (2006).

[26] J. Strümpfel and C. May, Vacuum 59, 500 (2000).

[27] Transparent Conductive Zinc Oxide, “Basics and applications in thin-film solar cells”, edited by K. Ellmer, A. Klein, and B. Rech (Springer, Berlin, 2008).

[28] P. Chelvanathan, et al., “Annealing effect in structural and electrical properties of sputtered Mo thin film”, Appl. Surf. Sci. (2014).

[29] M. Nastasi, J. Mayer, J.K. Hirvonen, "Ion-Solid interactions: fundamentals and applications," Cambridge Solid State Science Series, Cambridge University Press, Cambridge, UK (2004).

[30] J. Mater. Chem. A, 2017, 5,18299.

[31] T. J. Vink, M. A. J. Somers, J. L. C. Daams, and A. G. Driks, J. Appl. Phys. 70, 4301 (1991).

[32] Scherrer et al, “After sixty years: A survey and some new results in the determination of crystallite size,” J. Appl. Cryst. 11 (1978) p102-113.

[33] P. Chelvanathan, et al., Annealing effect in structural and electrical properties of sputtered Mo thin film, Appl. Surf. Sci. (2014).

Authorized licensed use limited to: UNIVERSITY TENAGA NASIONAL. Downloaded on November 24,2021 at 02:26:28 UTC from IEEE Xplore. Restrictions apply.